Binding Specificity of Multiprotein Signaling Complexes Is Determined by Both Cooperative Interactions and Affinity Preferences†

Jon C. D. Houtman,‡ Yuichiro Higashimoto,§ Nazzareno Dimasi,||,⊥ Sangwoo Cho,|| Hiroshi Yamaguchi,§ Brent Bowden,‡ Carole Regan,‡ Emilio L. Malchiodi,|| Roy Mariuzza,|| Peter Schuck,# Ettore Appella,§ and Lawrence E. Samelson*,‡

Laboratory of Cellular and Molecular Biology and Laboratory of Cell Biology, National Cancer Institute, and Protein Biophysics Resource, Division of Bioengineering and Physical Science, ORS, OD, National Institutes of Health, Bethesda, Maryland 20892, and Center for Advanced Research in Biotechnology, W. M. Keck Laboratory for Structural Biology, University of Maryland Biotechnology Institute, Rockville, Maryland 20850

Received September 24, 2003; Revised Manuscript Received February 6, 2004

ABSTRACT: The generation of multiprotein complexes at receptors and adapter proteins is crucial for the activation of intracellular signaling pathways. In this study, we used multiple biochemical and biophysical methods to examine the binding properties of several SH2 and SH3 domain-containing signaling proteins as they interact with the adapter protein linker for activation of T-cells (LAT) to form multiprotein complexes. We observed that the binding specificity of these proteins for various LAT tyrosines appears to be constrained both by the affinity of binding and by cooperative protein−protein interactions. These studies provide quantitative information on how different binding parameters can determine in vivo binding site specificity observed for multiprotein signaling complexes.

The formation of multiprotein complexes at receptors and adapter proteins brings enzymes to the site of active signal transduction and is vital for the activation of intracellular signaling pathways. Many signaling proteins in these complexes contain several association domains and binding motifs, which allows for the formation of multiple protein−protein interactions by a single protein. The individual interaction domains have affinity preferences for individual motifs, resulting in substantial in vivo binding specificity, i.e., binding of one signaling molecule to a specific site on a binding partner (*1*−*4*). Studies examining the affinity of peptide ligands for src homology 2 (SH2)[1] domains, which inducibly bind to protein motifs with phosphorylated tyrosine residues, and src homology 3 (SH3) domains, which constitutively bind to both proline-rich motifs (*5*) and arginine/lysine rich-motifs (*6*, *7*), have indicated that affinity may not be the only determinate in defining in vivo binding specificity (*5*). Increased affinity due to cooperativity, defined as alterations in affinity between two proteins due to the presence of other proteins and/or post-translational modifications, can increase the stability of multiprotein complexes, but it may also facilitate the binding of proteins to specific sites on another molecule. Even though there are multiple examples in the literature of how multipoint associations can lead to cooperative interactions between two proteins, less has been done to clarify how cooperative interactions can enhance or inhibit complex formation at various sites on receptors and adapter proteins. These questions ultimately address whether cooperative interactions can determine in vivo binding specificity of protein interactions within multiprotein signaling complexes.

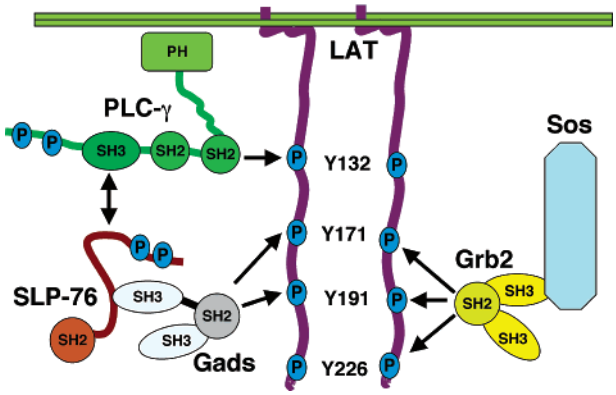

FIGURE 1: Model of protein complex formation at LAT. A representation of the present model for the binding of the Grb2/Sos complex, the Gads/SLP-76 complex, and PLC-γ to LAT tyrosines 132, 171, 191, and 226 is shown. Detectable associations are identified by the arrows.

LAT or linker for activation of T-cells is a 36−38 kDa integral membrane adapter protein that is vital for immunological function (*8*). Upon T-cell receptor (TCR) stimulation, LAT is rapidly phosphorylated on several conserved tyrosines and directly binds via SH2 domains to several proteins, such as Grb2, Gads, and PLC-γ, (Figure 1) (*9*, *10*). At the same time, Grb2 associates with Sos or

† R.M. is supported by grants from the Sandler Program for Asthma Research.

* To whom correspondence should be addressed. Phone: (301) 496-9683. Fax: (301) 496-8479. E-mail: samelson@helix.nih.gov.

‡ Laboratory of Cellular and Molecular Biology, National Cancer Institute.

§ Laboratory of Cell Biology, National Cancer Institute.

|| University of Maryland Biotechnology Institute.

⊥ Present address: Istituto Giannina Gaslini, Largo Gerolamo Gaslini 5, 16147 Genova, Italy.

Protein Biophysics Resource, Division of Bioengineering and Physical Science, National Institutes of Health.

[1] Abbreviations: SH2, src homology 2; SH3, src homology 3; LAT, linker for activation of T-cells; TCR, T-cell receptor; ITC, isothermal titration calorimetry; $\Delta H°$, change in enthalpy; $-T\Delta S°$, change in entropy; SE, sedimentation equilibrium analytical ultracentrifugation; SV, sedimentation velocity analytical ultracentrifugation; CD, circular dichroism; $\Delta G°$, change in free energy.

10.1021/bi0357311 CCC: $27.50
Published on Web 03/12/2004

Cbl, and Gads interacts with SLP-76, all via SH3 domain-induced interactions, thereby mediating the indirect binding of Sos, Cbl, and SLP-76 to LAT (Figure 1) (*9*, *10*).

Several structure/function investigations have examined which specific tyrosines on LAT mediate the in vivo association with Grb2, PLC-γ, and the Gads/SLP-76 complex (*11*−*14*). It was found that Grb2 binds phosphorylated LAT tyrosines 171, 191, and 226 but had little association with phosphorylated LAT tyrosine 132 (Figure 1) (*11*, *12*). In contrast, the Gads/SLP-76 complex principally binds to phosphorylated LAT tyrosine 191, with a reduced amount of binding to phosphorylated tyrosine 171 and no interaction with phosphorylated tyrosines 132 or 226 (Figure 1) (*11*, *12*). At the same time, PLC-γ preferentially interacts with phosphorylated LAT tyrosine 132 with no detectable binding to phosphorylated tyrosines 171, 191, or 226 (Figure 1) (*12*−*14*), an interaction that appears to be mediated primarily by the N-terminal SH2 domain of PLC-γ (*15*, *16*).

These studies also suggest that cooperative interactions may be important for the formation of multiprotein complexes on LAT upon TCR activation (*9*, *10*). For example, the mutation of LAT tyrosines 171, 191, and 226 results in a reduction of LAT/PLC-γ binding, suggesting that Grb2 or Gads binding is required to stabilize the association of PLC-γ and LAT (*12*). In support of this model, the presence of only LAT tyrosine 132 is not sufficient for the binding of PLC-γ to LAT whereas the presence of both LAT tyrosines 132 and 191 is sufficient (*11*). In addition, deletion of the putative PLC-γ binding site on SLP-76 results in the loss of binding between PLC-γ and SLP-76 (*17*). These data suggest that LAT, PLC-γ, Gads, and SLP-76 cooperatively form a multiprotein complex upon TCR activation (Figure 1) (*10*, *17*, *18*). However, none of the previous biochemical studies has directly defined the binding parameters between PLC-γ1 and the Gads/SLP-76 complex.

In this study, we used biophysical techniques to examine the affinity of PLC-γ, Grb2, Gads, and the Gads/SLP-76 complex for small phosphopeptides derived from LAT and to investigate the interaction of SLP-76 with Gads and/or PLC-γ in the absence of LAT. Our data suggest that the in vivo specificity of binding of Grb2 to LAT can be explained by substantial differences in affinity, whereas the association of the Gads/SLP-76 complex and PLC-γ with specific LAT tyrosines is not driven solely by affinity preferences. We also found that the affinity of Gads for SLP-76 is high at 25 °C. In contrast, PLC-γ did not have detectable binding to SLP-76 alone at this temperature. Interestingly, our data confirm that SLP-76 undergoes a substantial change in secondary structure upon binding Gads (*19*), an effect that appears to mediate the increased binding of PLC-γ to the Gads/SLP-76 complex compared to SLP-76 alone at higher temperatures. Together, these data indicate that the in vivo binding specificity observed at the LAT complex is determined by both affinity preferences and cooperative interactions.

EXPERIMENTAL PROCEDURES

Full-length mouse Gads was PCR amplified and cloned into the pT7-7 bacterial expression vector. The proline-rich domain of human SLP-76, corresponding to residues 157−420, and the SH2−SH2−SH3 domains of rat PLC-γ1, corresponding to residues 550−846, were PCR amplified and cloned into the pET-28a(+) bacterial expression vector (Novagen, Madison, WI). Mutation of tryptophan 586 to lysine in the SH3 domain (SH3 mutant) of PLC-γ1 was performed with the QuikChange site-directed mutagenesis kit (Stratagene, La Jolla, CA). The fidelity of all the constructs was confirmed by DNA sequencing.

During final preparation of this paper the expression construct for SLP-76 was found to have a phenylalanine to serine mutation at amino acid 342. The F342S mutation is at least 100 amino acids outside of the core binding motifs for both PLC-γ and Gads. Functional studies performed over the past 8 years with this construct indicate that this mutation has no effect on SLP-76 biological activity.

Protein Purification. (A) Grb2 Purification. Sf-9 cells expressing full-length Grb2 were lysed and partially purified using a 300VHP81010 Q anion-exchange column (Vydac, Hesperia, CA). The elute was applied to an NHS-activated HP column (Amersham Biosciences, Piscataway, NJ) containing a CD45-derived phosphopetide that binds to Grb2 (*20*). Grb2 was eluted from the column with phenyl phosphate and dialyzed three times against 1× PBS with 2.5 mM DTT. The purified Grb2 was >95% pure as assessed by PAGE analysis.

(B) Gads Purification. Insoluble inclusion bodies were purified from Gads-expressing BL-21(DE3) cells (Novagen, Madison, WI) and solubilized with 8 M urea. The solubilized inclusion bodies were refolded by dilution, concentrated, and then applied to an NHS-activated HP column containing a CD45-derived phosphopetide (*20*). Gads was eluted from the column with phenyl phosphate and dialyzed three times against 1× PBS with 2.5 mM DTT. The purified Gads was >95% pure as assessed by PAGE analysis.

(C) SLP-76 Fragment Purification. SLP-76-expression BL-21(DE3) cells were lysed by sonication, and the supernatant was applied to a Ni^{2+}-loaded HiTrap chelating HP column (Amersham Biosciences, Piscataway, NJ). The SLP-76 fragment was further purified using a 16/60 Superdex 200 column (Amersham Biosciences, Piscataway, NJ) that was equilibrated with 1× PBS and then dialyzed against 1× PBS. The purified SLP-76 fragment was >95% pure as assessed by PAGE analysis.

(D) Gads/SLP-76 Complex Purification. Partially purified Gads and the SLP-76 fragment were stirred at 4 °C for 1 h and then applied to an NHS-activated HP column containing a CD45-derived phosphopetide (*20*). The Gads/SLP-76 complex was further purified using a 16/60 Superdex 200 column that was equilibrated with 1× PBS with 2.5 mM DTT. The purified Gads/SLP-76 complex was dialyzed against 1× PBS with 2.5 mM DTT and was >95% pure as assessed by PAGE analysis.

(E) PLC-γ Fragment Purification. Inclusion bodies from PLC-γ-expressing BL-21(DE3) cells were solubilized with 8 M urea. The solubilized inclusion bodies were applied to a Ni^{2+}-loaded HiTrap chelating HP column, and the bound PLC-γ was refolded on the column. The purified PLC-γ was then dialyzed three times against 1× PBS with or without 2.5 mM DTT. The purified PLC-γ was >95% pure as assessed by PAGE analysis.

Peptide Synthesis. Peptides were synthesized by the solid-phase method with Fmoc chemistry with phosphotyrosine incorporated as Fmoc-Tyr(PO_3H_2)-OH (Novabiochem, San

Diego, CA). The peptides were purified by HPLC, and the mass of peptides was confirmed by MALDI-TOF mass spectrometry (Micromass, Manchester, U.K.).

Isothermal Titration Calorimetry. ITC measurements were performed using a VP-ITC calorimeter (MicroCal, Northhampton, MA). Titrations were performed in 1× PBS, pH 7.4 (SLP-76 and PLC-γ), or 1× PBS, pH 7.4, with 2.5 mM DTT (Grb2, Gads, Gads/SLP-76 complex, SLP-76, and PLC-γ). The concentrations of the injected peptides and proteins were measured by A_{276}. The protein and peptide solutions were degassed before each experiment. Heats of dilution were subtracted from the raw data. All injections fit the single binding site mechanism with 1:1 stoichiometry and were repeated three to five times. The values for the stoichiometry of binding and thermodynamic constants were determined using the ORIGIN software package provided by the VP-ITC calorimeter manufacturer using the equations listed below.

The total heat content Q of the interaction of two solutes, A and B, in can be described as

$$Q = \frac{nM_t\Delta H^\circ V_0}{2}\left[1 + \frac{X_t}{nM_t} + \frac{1}{nK_AM_t} - \sqrt{\left(1 + \frac{X_t}{nM_t} + \frac{1}{nK_AM_t}\right)^2 - \frac{4X_t}{nM_t}}\right] \quad (1)$$

where K_A is the equilibrium association constant, n is the stoichiometry of binding, ΔH° is the change in molar enthalpy upon binding, V_0 is the active volume of the reaction cell, M_t is the total concentration of receptor (A) in V_0, and X_t is the total concentration of ligand (B) in V_0 (*21*). The experimentally observed quantity is the change in Q resulting from a series of injections i of B (of a volume ΔV_i) into the volume initially containing A. The observed heat of the ith injection can be expressed as

$$\Delta Q(i) = Q(i) + \frac{\Delta V_i}{V_0}\left(\frac{Q(i) + Q(i-1)}{2}\right) - Q(i-1) \quad (2)$$

including a correction for the increase in reaction volume with each injection. Using eqs 1 and 2, the values of n, ΔH°, and K_A were solved by least-squares analysis using standard Marquardt methods. The values for the change in free energy (ΔG°) and the change in entropy (ΔS°) were then calculated as

$$\Delta G^\circ = -RT \ln K_A = \Delta H^\circ - T\Delta S^\circ \quad (3)$$

where R denotes the gas constant and T is the absolute temperature. The equilibrium association constant K_A was also expressed as an equilibrium dissociation constant $K_D = 1/K_A$.

Analytical Ultracentrifugation. Sedimentation equilibrium experiments were conducted at 4 °C in an Optima XLI/A (Beckman Coulter, Fullerton, CA) at rotor speeds of 20000, 25000, and 30000 rpm in double-sector Epon centerpieces. Both absorbance data at 280 nm and interference optical fringe displacement data were acquired. Global nonlinear regression was performed using SEDPHAT (*23*), using the equations for the radial concentration distribution of two ideally sedimenting species in mechanical and chemical equilibrium

$$\alpha(r) = c_A\epsilon_A d \exp\left[M^*_A\frac{\omega^2(r^2 - r_0^2)}{2RT}\right] + c_B\epsilon_B d \exp\left[M^*_B\frac{\omega^2(r^2 - r_0^2)}{2RT}\right] + K_Ac_Ac_B(\epsilon_A + \epsilon_B)d \exp\left[(M^*_A + M^*_B)\frac{\omega^2(r^2 - r_0^2)}{2RT}\right] \quad (4)$$

where $\alpha(r)$ is the experimentally observed absorbance at distance r from the center of rotation, c_A and c_B are the molar concentrations of species A and B at the reference radius r_0, ϵ_A and ϵ_B are both species molar extinction coefficients, d is the optical path length, M^*_A and M^*_B are the buoyant molar masses of the species A and B, respectively, K_A is the equilibrium association constant, ω is the angular velocity, R is the gas constant, and T is the absolute temperature (*22*, *23*). The buoyant molar mass values of all species were predetermined by sedimentation experiments of each species alone and fitting the above eq 4 to the observed absorbance profiles, setting c_B zero. For all proteins, the buoyant molar mass values were found to be consistent with those predicted by the amino acid composition, within the uncertainty of the compositional partial specific volume (*22*). Both SLP-76 and PLC-γ and the mixture were found to be well described with models conserving total mass, with the bottom position of the solution column determined by nonlinear regression, as described in detail in ref *24*.

Sedimentation velocity experiments were conducted at a rotor speed of 50000 or 55000 rpm at rotor temperatures of 4 and 19 °C. Interference fringe displacement profiles were analyzed with SEDFIT, using a model for continuous sedimentation coefficient distributions $c(s)$ (*25*). In brief, the experimental data $a(r,t)$ were modeled as superpositions

$$\alpha(r,t) \cong \int_{s_{min}}^{s_{max}} c(s)\chi(s,D(s),r,t)\,ds + \alpha_{TI}(r) + \alpha_{RI}(t) + \epsilon \quad (5)$$

of solutions of the Lamm equation

$$\frac{\partial\chi}{\partial t} = \frac{1}{r}\frac{\partial}{\partial r}\left[rD\left(\frac{\partial\chi}{\partial r}\right) - s\omega^2r^2\chi\right] \quad (6)$$

(*26*), calculated by finite element methods (*27*). The diffusion coefficients D were estimated through a weight-average frictional ratio f/f_0 as

$$D(s) = \frac{\sqrt{2}}{18\pi}\kappa Ts^{-1/2}(\eta(f/f_0)_w)^{-3/2}((1 - \bar{v}\rho)/\bar{v})^{-1/2} \quad (7)$$

(*28*). The time-invariant signal contributions $\alpha_{TI}(r)$ and the radial-invariant offsets $\alpha_{RI}(t)$ were calculated by algebraic noise decomposition (*29*). The integral equation was solved with maximum entropy regularization. A detailed description of the resolution and performance of this approach can be found in ref *25*. The weight-average frictional ratio and the meniscus position of the sample were optimized by nonlinear regression, leading to final rms errors of the sedimentation model of ~0.004 fringes.

Circular Dichroism. CD spectra were measured in a Jasco J-810 spectropolarimeter (Jasco Inc., Easton, MD) at temperatures of 4 and 30 °C, using rectangular quartz cuvettes

Table 1: Thermodynamic Parameters for the Association of PhosphoLAT Peptides with SH2 Domain-Containing Proteins[a]

peptide	K_b (M^{-1})	K_d (nM)	$\Delta H°$ (kcal/mol)	$-T\Delta S°$ (kcal/mol)	$\Delta G°$ (kcal/mol)
(A) Grb2					
pLAT 132	ND	ND	ND	ND	ND
pLAT 171	$3.68 \pm 0.50 \times 10^6$	272	-8.34 ± 1.20	0.59 ± 1.14	-8.93 ± 0.09
pLAT 191	$12.62 \pm 0.47 \times 10^6$	79	-8.12 ± 0.76	-1.57 ± 0.76	-9.69 ± 0.02
pLAT 226	$5.76 \pm 0.78 \times 10^6$	174	-12.03 ± 1.51	2.83 ± 1.48	-9.20 ± 0.09
(B) Gads					
pLAT 132	ND	ND	ND	ND	ND
pLAT 171	$6.09 \pm 1.23 \times 10^6$	164	-9.57 ± 0.64	0.34 ± 0.51	-9.23 ± 0.13
pLAT 191	$6.60 \pm 1.12 \times 10^6$	152	-7.34 ± 0.30	-1.95 ± 0.31	-9.29 ± 0.11
pLAT 226	$2.44 \pm 0.22 \times 10^6$	410	-4.03 ± 0.65	-4.68 ± 0.70	-8.71 ± 0.05
(C) Gads/SLP-76					
pLAT 132	ND	ND	ND	ND	ND
pLAT 171	$5.84 \pm 0.93 \times 10^6$	171	-9.05 ± 1.23	-0.15 ± 1.30	-9.20 ± 0.12
pLAT 191	$7.30 \pm 1.12 \times 10^6$	137	-7.93 ± 0.34	-1.40 ± 0.32	-9.33 ± 0.11
pLAT 226	$2.68 \pm 0.80 \times 10^6$	373	-3.94 ± 0.60	-4.78 ± 0.76	-8.72 ± 0.16
(D) PLC-γ					
pLAT 132	$16.16 \pm 4.60 \times 10^6$	62	-15.73 ± 0.28	5.96 ± 0.32	-9.77 ± 0.19
pLAT 171	$1.80 \pm 0.07 \times 10^6$	556	5.61 ± 0.22	-14.15 ± 0.20	-8.54 ± 0.02
pLAT 191	$1.63 \pm 0.19 \times 10^6$	615	-7.76 ± 0.37	-0.70 ± 0.44	-8.46 ± 0.07
pLAT 226	$1.75 \pm 0.20 \times 10^6$	570	4.01 ± 0.30	-12.52 ± 0.25	-8.51 ± 0.06

[a] Titrations were performed and analyzed as described in Experimental Procedures with representative binding isotherms shown in Figure 3A,B. No binding to nonphosphorylated peptides was observed. ND = no detectable binding.

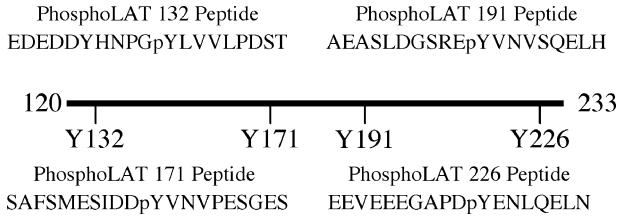

FIGURE 2: Phosphopeptides derived from LAT. Phosphopeptides corresponding to the regions surrounding LAT tyrosines 132, 171, 191, and 226 were synthesized as described in Experimental Procedures.

of 1 or 2 mm path length, respectively, with a protein concentration of 0.15 mg/mL. Data shown are averages of three measurements, each made at a scan speed of 100 nm/min with a time constant of 2 s.

RESULTS

Phosphorylated and nonphosphorylated 18−20 amino acid peptides that correspond to the protein−protein interaction sites on LAT, as defined by previous in vivo binding studies, were synthesized and purified. These peptides contain the in vivo binding sites for PLC-γ (phosphoLAT 132 peptide), Grb2 (phosphoLAT 171, 191, and 226 peptides), and Gads (phosphoLAT 171 and 191 peptides) (Figure 2). We then examined the binding of the four phosphoLAT peptides to a fragment of PLC-γ (encompassing the SH2−SH2−SH3 domains of PLC-γ1), full-length Grb2, full-length Gads, and the physiologically relevant complex formed between Gads and the proline-rich section of SLP-76 (encompassing amino acids 158−421). The affinity of these peptides for the purified signaling proteins was determined using isothermal titration calorimetry (ITC), a method that measures stoichiometry, binding constants, and thermodynamic parameters in a single reaction.

As seen in Table 1, the equilibrium dissociation constants of Grb2, Gads, and the Gads/SLP-76 complex for the phosphoLAT 171, 191, and 226 peptides ranged between $K_d = 79-410$ nM. As expected, these proteins did not have detectable binding to the phosphoLAT 132 peptide (Table 1A−C). From the protein concentrations used for these experiments and the detection limit of the calorimeter, the binding of Grb2, Gads, and the Gads/SLP-76 complex with the phosphoLAT 132 peptide is estimated to be at least 50−100-fold weaker than for the binding of these proteins to the phosphoLAT 171, 191, and 226 peptides. The interaction of Grb2, Gads, and the Gads/SLP-76 complex with the phosphoLAT 171, 191 and 226 peptides is exothermic with favorable, negative change in enthalpy ($\Delta H°$) values and low change in entropy ($-T\Delta S°$) values (Figure 3A and Table 1A−C), a thermodynamic pattern similar to previously published SH2 domain/phosphopeptide interactions (*30*−*34*). There was no detectable association of Grb2, Gads, or the Gads/SLP-76 complex with nonphosphorylated LAT peptides (data not shown). Taken together, these data indicate that, although Grb2, Gads, and the Gads/SLP-76 complex may have an affinity preference for phosphorylated LAT tyrosines 171, 191, and 226 compared to phosphorylated LAT tyrosine 132, these proteins do not appear to have a substantial difference in affinity between phosphorylated LAT tyrosines 171, 191, and 226.

As determined by ITC, PLC-γ bound to the phosphoLAT 132 peptide with a $K_d = 62$ nM, whereas the K_d for the phosphoLAT 171, 191, and 226 peptides ranged between 556 and 615 nM (Table 1D). The binding of PLC-γ to the phosphoLAT 132 and 191 peptides is exothermic with large, negative values for $\Delta H°$ (Table 1D) whereas the binding to the phosphoLAT 171 and 226 peptides is endothermic with large, negative $-T\Delta S°$ values and unfavorable $\Delta H°$ values (Figure 3B and Table 1D). There was no detectable binding of PLC-γ to the nonphosphorylated LAT peptides (data not shown). These data suggest that PLC-γ binds ~10-fold better to its preferred in vivo binding site, phosphorylated LAT tyrosine 132, compared to phosphorylated LAT tyrosines 171, 191, and 226, although a 10-fold difference in affinity may not be substantial enough to account for the preference of PLC-γ for phosphorylated LAT tyrosine 132.

The binding studies presented above indicate that large affinity differences may not be the sole determinant for the

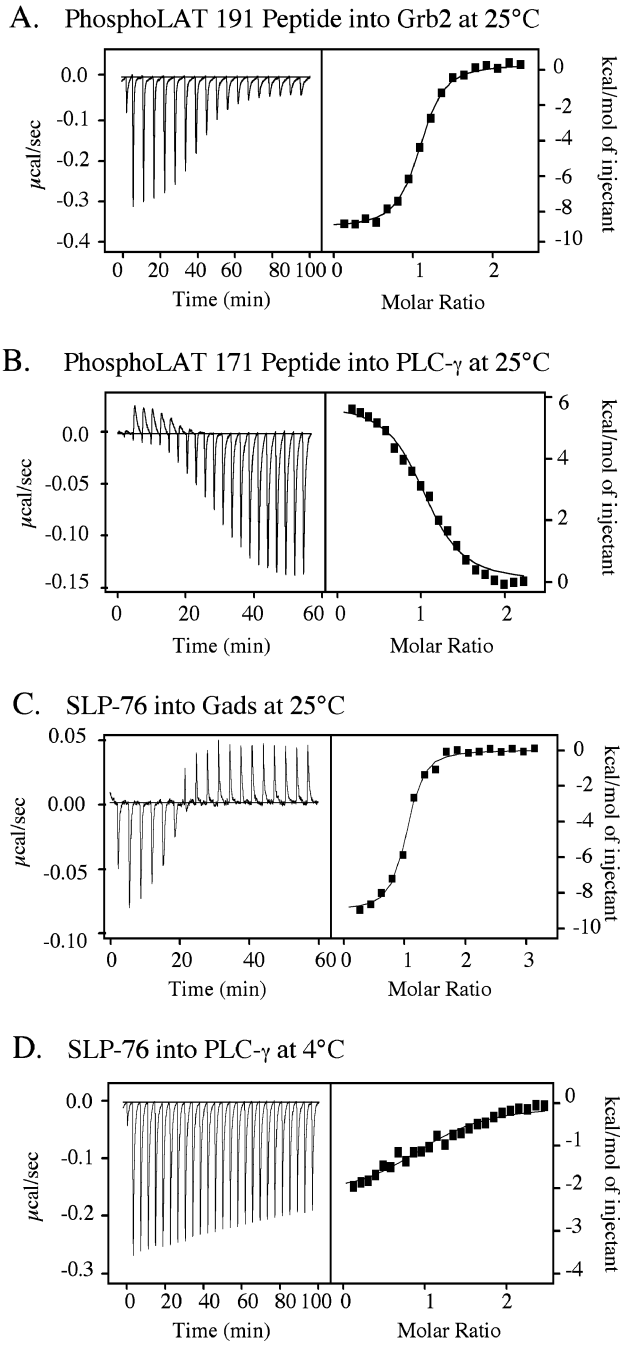

FIGURE 3: Representative binding isotherms for the interaction of Grb2 and PLC-γ with the phosphoLAT peptides and for the binding of SLP-76 to Gads and PLC-γ. The data were fit to eqs 1 and 2 as described in Experimental Procedures. The best-fit values for n, $\Delta H°$, and K_b were determined by nonlinear regression. The values for $-T\Delta S°$ and $\Delta G°$ were then calculated using eq 3. All data fit a single binding site mechanism with a 1:1 binding stoichiometry. (A) The injection of phosphoLAT 191 into Grb2. The titration involved the injection of 17−8 μL aliquots of the phosphoLAT 191 peptide (100 μM) into Grb2 (4.5 μM). The experiment was performed at 25 °C in 1× PBS (pH 7.4) with 2.5 mM DTT. (B) The injection of phosphoLAT 171 into PLC-γ. The titration involved the injection of 20−14.5 μL aliquots of the phosphoLAT 171 peptide (100 μM) into PLC-γ (10 μM). The experiment was performed at 25 °C in 1× PBS (pH 7.4) with 2.5 mM DTT. (C) The injection of SLP-76 into Gads. The titration involved the injection of 17−3.25 μL aliquots of the SLP-76 fragment (91 μM) into Gads (1.2 μM). The experiment was performed at 25 °C in 1× PBS (pH 7.4) with 2.5 mM DTT. (D) The injection of SLP-76 into PLC-γ. The titration involved the injection of 24−9 μL aliquots of the SLP-76 fragment (100 μM) into PLC-γ (6 μM). The experiment was performed at 4 °C in 1× PBS (pH 7.4).

in vivo binding specificity observed at the LAT complex and suggest that cooperative effects from the formation of multiprotein complexes may contribute in targeting these signaling molecules to specific phosphorylated LAT tyrosines. Several recent studies have suggested that while bound to LAT, PLC-γ associates with the Gads/SLP-76 complex via a SH3 domain-mediated interaction (*11*, *12*, *17*). However, none of these studies have directly measured the binding parameters of these interactions. Therefore, we decided to use several biophysical techniques to examine the interaction of PLC-γ, Gads, and SLP-76 in the absence of LAT to determine which interactions are physiologically relevant.

As assessed by ITC, the interaction of Gads with the 265 amino acid SLP-76 fragment is of high affinity (K_d = 19 nM) and is enthalpically driven (Figure 3C and Table 2). This is one of the strongest reported affinities for a SH3 domain/ligand interactions (*5*) and is 5−10-fold stronger than that reported for the binding of the C-terminal SH3 domain of Gads to a 10 amino acid peptide derived from the core binding motif of SLP-76 (*7*, *35*). PLC-γ did not have detectable binding at 25 °C to the SLP-76 fragment (Table 2), suggesting that the K_d of these proteins at this temperature is greater than 40 μM. The recombinant PLC-γ did bind at 25 °C to a high-affinity peptide ligand derived from phage display experiments (*36*) with a K_d of 1 μM (data not shown), indicating that the SH3 domain of the PLC-γ fragment was fully functional at these temperatures. To test whether the interaction of PLC-γ with SLP-76 can be detected if the entropic penalty of binding is lowered, we examined this interaction at 4 °C. Interestingly, we found that at 4 °C this interaction was both enthalpically and entropically driven with a K_d of 3.3 μM (Figure 3D and Table 2).

To more fully test the interaction between the PLC-γ fragment and the SLP-76 fragment, this association was further examined using analytical ultracentrifugation (*22*, *23*). The experimental concentration distributions from sedimentation equilibrium analytical ultracentrifugation (SE) (Figure 4A) at 4 °C fit best to a binding model that assumed an interaction between PLC-γ and the SLP-76 fragment (Figure 4A, solid line), with an estimated K_d of 20 μM or smaller, which is consistent with the values determined by ITC (Table 2). In contrast, the data were incompatible with the binding model that assumed no interaction (Figure 4A, dashed line). The temperature-dependent nature for the interaction of PLC-γ with SLP-76 was confirmed by sedimentation velocity analytical ultracentrifugation (SV). Consistent with the previous SE and ITC experiments, the sedimentation coefficient distributions showed significant complex formation between PLC-γ and SLP-76 at 4 °C but little complex formation at 20 °C (data not shown). The data presented above suggest that, in the absence of LAT, the interaction of SLP-76 with Gads occurs readily at physiological temperatures, whereas the interaction of SLP-76 with PLC-γ may not occur at these temperatures.

Protein−protein interactions that have temperature-dependent differences in affinity often have changes in secondary structure during the binding reaction. The experiments presented above suggest that the interaction of SLP-76 with PLC-γ may involve a substantial change in the secondary structure of either protein. This conclusion is supported by previous work by Liu and co-workers that demonstrated that

Table 2: Thermodynamic Parameters for the Association of the SLP-76 Fragment with Gads and PLC-γ[a]

protein	temp (°C)	K_b (M^{-1})	K_d (nM)	$\Delta H°$ (kcal/mol)	$-T\Delta S°$ (kcal/mol)	$\Delta G°$ (kcal/mol)
binding to SLP-76						
Gads	25	$52.81 \pm 2.21 \times 10^6$	19	-12.03 ± 1.72	1.65 ± 1.80	-10.38 ± 0.25
PLC-γ	25	ND	ND	ND	ND	ND
PLC-γ	4	$0.30 \pm 0.01 \times 10^6$	3345	-1.77 ± 0.05	-5.57 ± 0.06	-7.34 ± 0.01

[a] Titrations were performed and analyzed as described in Experimental Procedures with representative binding isotherms shown in Figure 3C,D. ND = no detectable binding.

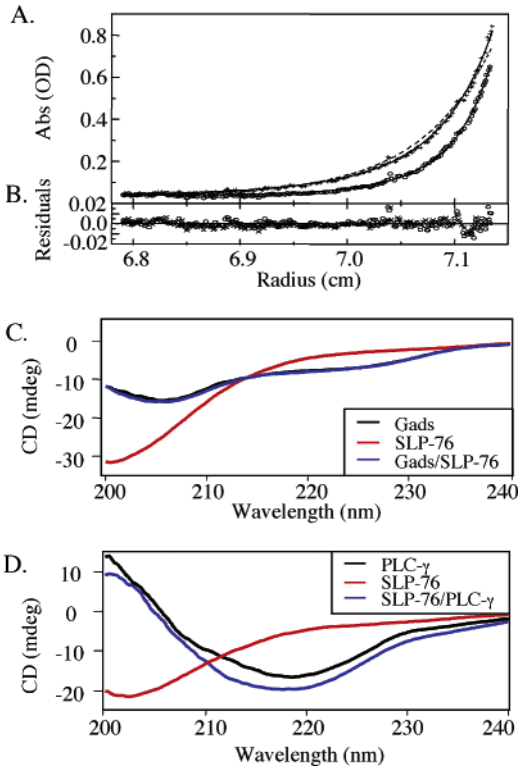

FIGURE 4: Analytical ultracentrifugation and circular dichroism analysis of SH3 domain-mediated interactions. (A) Absorbance profile of a mixture of SLP-76 and PLC-γ in sedimentation equilibrium at 20000 (+) and 25000 rpm (○) at 4 °C. The solid line is the best global with eq 4 and $K_A > 5 \times 10^4$/M; the dashed line indicates a model that assumes no binding between PLC-γ and SLP-76 (eq 4 with $K_A = 0$), for clarity shown only for the 20000 rpm data. (B) Residuals of the best fit. (C) CD spectra of Gads (black line), SLP-76 (red line), and a mixture of Gads and SLP-76 (blue line) at 0.15 mg/mL acquired at 4 °C. (D) CD spectra of SLP-76 (red line), PLC-γ (black line), and a mixture of SLP-76 and PLC-γ (blue line) at 0.15 mg/mL acquired at 4 °C.

a short peptide derived from SLP-76 containing the core binding motif for Gads undergoes a change in secondary structure upon binding the C-terminal SH3 domain of Gads (*19*). To determine whether the entire proline-rich region of SLP-76 undergoes a change in secondary structure upon binding Gads and/or PLC-γ, we acquired the circular dichroism (CD) spectra of mixtures of these proteins at 4 °C. As expected from the presence of SH2 and SH3 domains, both Gads (Figure 4C, black line) and the PLC-γ fragment (Figure 4D, black line) had significant secondary structure. In contrast, the CD spectrum of SLP-76 (Figure 4C,D, red line) was indicative of an unordered polypeptide (red line) (*37*). Interestingly, the Gads/SLP-76 mixture (Figure 4C, blue line) and the PLC-γ/SLP-76 mixture (Figure 4D, blue line) had substantial secondary structure that was similar to the extent of secondary structure of Gads and PLC-γ alone, indicating that the proline-rich region of SLP-76 had undergone a substantial change in secondary structure upon binding to either Gads or PLC-γ.

Potentially, the structural transition described above could mediate cooperativity, with the binding of PLC-γ to SLP-76 occurring more readily if SLP-76 is structurally stabilized by its association with Gads, an interaction that is highly favorable at physiological temperatures (Table 2). Unfortunately, neither the Gads/SLP-76 complex nor the PLC-γ fragment could be concentrated sufficiently to allow for this interaction to be analyzed by ITC. Therefore, we examined the binding of PLC-γ to the Gads/SLP-76 complex at 19 °C using SV analytical ultracentrifugation under conditions where PLC-γ showed little binding to SLP-76 alone (data not shown). As seen in Figure 5A, the Gads/SLP-76 complex (orange line) sedimented with a single peak at 3.1 S, faster than either the wild-type PLC-γ fragment at 2.8 S (green line) or the SH3 domain-mutated PLC-γ fragment at 2.7 S (purple line). In the same experiment, the sedimentation coefficient distribution obtained from an equimolar mixture of the Gads/SLP-76 complex and wild-type PLC-γ, each at 5 μM (Figure 5B, black line), showed a single peak of 3.1 S, which reflects a weight-average sedimentation of all species and complexes formed. As described previously (*38*), for mixtures of protein components with interactions on the time scale of sedimentation, the resulting peaks in $c(s)$ reflect average s-values in a concentration-dependent manner. Importantly, in the present case, the peak position observed is at a higher sedimentation rate than the average sedimentation values for the unbound proteins, indicating the presence of a faster sedimenting complex. This is confirmed by an analogous experiment with the SH3 domain-mutated PLC-γ under otherwise identical conditions (Figure 5B, blue line), which results in a $c(s)$ peak at 2.9 S, which is an average of the sedimentation values for the Gads/SLP-76 complex and the mutated PLC-γ fragment. To study the complex formation further, we conducted sedimentation velocity experiments at higher protein concentrations that create an increased population of the complex. The $c(s)$ mixture of the Gads/SLP-76 complex and the wild-type PLC-γ at 9 μM (Figure 4B, red line) resolves into three distinct species of 2.9, 3.1, and a now clearly resolved peak at 3.7 S. In contrast, the mixture of the Gads/SLP-76 complex and the PLC-γ SH3 mutant sedimented into a single distinct peak of 2.9 S (data not shown). Although these protein complexes could not be recovered and examined, the sedimenting species at 3.7 S is almost certainly a trimolecular complex between wild-type PLC-γ and the Gads/SLP-76 complex, since the equivalent peak is not observed for the mixture of the Gads/SLP-76 complex and the SH3 domain-mutated PLC-γ. The peaks at 2.9 and 3.1 S are likely an average of the unbound species, since these peaks correspond well with what was observed when these interactions were examined at lower protein

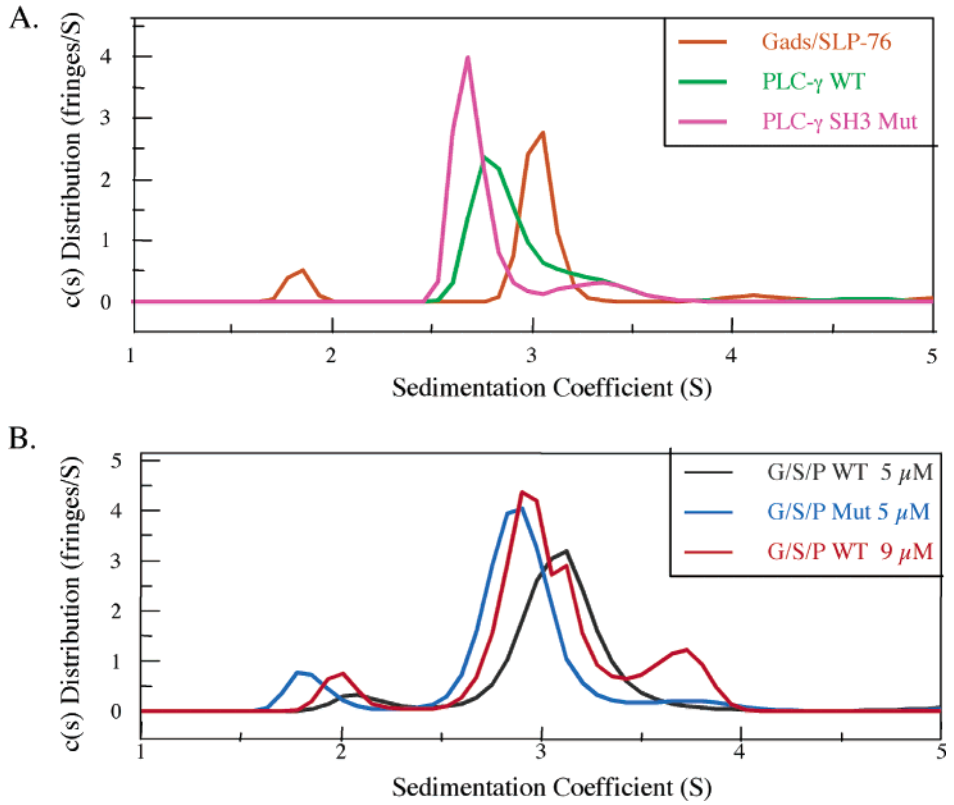

FIGURE 5: Analytical ultracentrifugation analysis of the association of PLC-γ with the Gads/SLP-76 complex. (A) Sedimentation coefficient distributions of the Gads/SLP-76 complex (orange line), wild-type PLC-γ (green line), and SH3 domain-mutated PLC-γ (purple line). The concentration of each protein or complex was 5 μM, and the experiment was performed at 19 °C. (B) Sedimentation coefficient distributions of an equimolar mixture of the Gads/SLP-76 complex and wild-type PLC-γ each at 5 μM (black line) or at 9 μM (red line) and an equimolar mixture of the Gads/SLP-76 complex and SH3 domain-mutated PLC-γ each at 5 μM (blue line). The experiment was performed at 19 °C.

concentrations. The separation of the peak for the trimeric complex when it is more populated and the observation of an average, unresolved peak when it is less populated are in line with the known properties of the *c*(*s*) distribution (*38*) and the maximum entropy regularization when applied to a reacting system. Together, these data show unambiguously that, in the absence of LAT, PLC-γ can interact with the Gads/SLP-76 complex at higher temperatures, an association that would likely be further stabilized upon binding to LAT.

DISCUSSION

In these studies, the affinity of LAT phosphopeptides for recombinant PLC-γ, Grb2, Gads, and the Gads/SLP-76 complex was determined using ITC. There was no substantial difference in the affinity of Grb2, Gads, and the Gads/SLP-76 complex for the phosphoLAT 171, 191, and 226 peptides, but these proteins show an at least 50−100-fold weaker binding for the phosphoLAT 132 peptide (Table 3). In contrast, PLC-γ bound approximately 10-fold stronger to the phosphoLAT 132 peptide compared to the phosphoLAT 171, 191, and 226 peptides (Table 3). These findings are not surprising for Grb2 since previous studies have demonstrated that Grb2 binds to phosphorylated LAT tyrosines 171, 191, and 226 but does not associate with phosphorylated LAT tyrosine 132 (Table 3) (*12*, *13*). However, for the association of PLC-γ and the Gads/SLP-76 complex with LAT, these findings are unexpected. From previous in vivo binding studies, the Gads/SLP-76 complex appears to preferentially associate with phosphorylated LAT tyrosine 191 (Table 3), whereas PLC-γ binds exclusively to phosphorylated LAT tyrosine 132 (Table 3) (*12*−*14*). Our studies suggest that affinity differences do not play a role in the preferential in vivo binding of the Gads/SLP-76 complex to phosphorylated LAT tyrosine 191 instead of phosphorylated LAT tyrosines 171 and 226, although they most likely explain the lack of binding to phosphorylated LAT tyrosine 132. Similarly, although PLC-γ has an affinity preference for phosphorylated LAT tyrosine 132 compared to other phosphorylated LAT tyrosines, a 10-fold difference in affinity may not be substantial enough to fully explain why PLC-γ specifically binds to phosphorylated LAT tyrosine 132 in vivo. Interestingly, even though the PLC-γ fragment used in these studies

Table 3: Comparison of in Vivo Structure/Function Studies and ITC Binding Studies[a]

		pY132	pY171	pY191	pY226
Grb2	in vivo	−	+++	+++	+++
	ITC	−	+++	+++	+++
Gads	in vivo	−	+	+++	−
	ITC	−	+++	+++	+++
PLC-γ	in vivo	+++	(+)	(+)	−
	ITC	+++	++	++	++

[a] The binding of Grb2, Gads, and PLC-γ to phosphorylated LAT tyrosines 132, 171, 191, and 226, derived from various structure/function studies and the ITC binding studies presented in this paper. For the in vivo structure/function studies, the number of plus marks (+) indicates the apparent contribution to in vivo binding, the plus mark in parentheses [(+)] indicates a contribution to stable binding not due to a direct interaction, and minus marks (−) indicated no detectable association. For the ITC binding studies, the relative values for K_d are indicated by the number of plus marks (+), with no detectable binding indicated by a minus mark (−).

contains two intact SH2 domains, this protein bound to the phosphoLAT peptides with a 1:1 stoichiometry. This corresponds well with previous in vivo structure/function data that has shown that only the N-terminal SH2 domain of PLC-γ is required for the association of this protein with phosphorylated LAT (*15*, *16*). These data, taken together, suggest that large differences in the affinity of SH2 domain-containing proteins for specific phosphorylated LAT tyrosines are not the only determinate in the substantial binding specificity that is observed in vivo. Interestingly, it appears that SH2 domains may have two thermodynamically distinct modes of phosphopeptide binding, one that is driven by changes in enthalpy and a second that is driven by changes in entropy. It is unclear whether this indicates two separate mechanisms for the binding of PLC-γ to phosphopeptide ligands or whether other factors are involved. However, the binding constants for the interaction of PLC-γ to the phosphoLAT 191 peptide, which is driven by entropy changes, and to the phosphoLAT 171 and 226 peptides, which are driven by changes in enthalpy, are similar, indicating that these two thermodynamically distinct modes of binding are most likely physiologically indistinguishable.

If the affinity is not the only driving force behind the in vivo binding specificity that is observed at the phosphorylated LAT complex, what is? Several factors may play a role in targeting PLC-γ and the Gads/SLP-76 complex to specific phosphorylated LAT tyrosines. For example, full-length PLC-γ may be positioned near phosphorylated LAT tyrosine 132 via the association of its PH domains with the plasma membrane (Figure 1). However, cooperative effects from the formation of multiprotein complexes may not only increase the affinity of PLC-γ and the Gads/SLP-76 complex for phosphorylated LAT but could help to target PLC-γ to phosphorylated LAT tyrosine 132 and the Gads/SLP-76 complex to phosphorylated LAT tyrosine 191 (Figure 1).

Since the interaction of SLP-76 with PLC-γ and/or Gads appears to be important for determining in vivo binding specificity at the LAT complex, the associations of these proteins were examined using multiple biophysical techniques. We found that Gads bound to the proline-rich region of SLP-76 with a K_d of 19 nM, which represents a 5−10-fold stronger binding than what was reported for the binding of the C-terminal SH3 domain of Gads to a 10 amino acid fragment of SLP-76 that encompasses the core-binding motif for these proteins (*7*, *35*). The difference in the binding constants observed in our study and in the previous studies is likely due to our use of full-length Gads and a large fragment of SLP-76, which suggests that contacts outside of the core binding motif may additionally stabilize the interaction of Gads with SLP-76. Surprisingly, when measured by ITC, we found that an interaction between PLC-γ and SLP-76 was only detectable when examined at 4 °C, suggesting that this interaction may not occur readily at physiological temperatures. These findings were confirmed by sedimentation velocity ultracentrifugation, where substantial binding between these proteins was observed when the experiments were performed at 4 °C but not when performed at 20 °C.

What could account for the temperature-dependent binding of PLC-γ to SLP-76? One possible reason for temperature-dependent alterations in affinity for protein−protein interactions can be the entropic effect of structural changes. When the secondary structure of Gads, PLC-γ, and SLP-76, both alone and in combination, was examined by circular dichroism, we observed that SLP-76 underwent a change in secondary structure from an unordered polypeptide to a more structured protein upon binding to either Gads or PLC-γ. This structural change has been observed previously for the binding of the Gads C-terminal SH3 domain to a short peptide containing the core binding motif from SLP-76 (*19*). These data show that the proline-rich domain of SLP-76 undergoes a substantial change in secondary structure upon binding to either Gads or PLC-γ.

The very strong binding between Gads and SLP-76 at 25 °C indicates that, while bound to Gads, SLP-76 will be structured at this temperature. This may facilitate the binding between PLC-γ and SLP-76 at higher, more physiological temperatures. This hypothesis was confirmed when the binding of PLC-γ to the Gads/SLP-76 complex was examined by sedimentation velocity ultracentrifugation. We observed a measurable interaction between wild-type PLC-γ and the Gads/SLP-76 complex at 19 °C, a result that was not seen when a SH3 domain-mutated PLC-γ was used. These data suggest that, when bound to Gads, SLP-76 forms a more structured state that greatly increases its affinity for PLC-γ at physiological temperatures. This cooperative interaction will most likely be stabilized when both PLC-γ and the Gads/SLP-76 complex are bound to phosphorylated LAT.

In conclusion, we have shown that substantial affinity differences appear to be important for targeting Grb2 to specific phosphorylated LAT tyrosines but that, in contrast, the in vivo binding specificity of PLC-γ and the Gads/SLP-76 complex was not governed only by affinity differences. Interestingly, in the absence of LAT, we found that Gads can readily bind to SLP-76 at 25 °C while PLC-γ had increased affinity to the Gads/SLP-76 complex compared to SLP-76 alone at these temperatures. Together, these data indicate that the cooperative multiprotein complex between PLC-γ and the Gads/SLP-76 complex may be targeted to specific phosphorylated LAT tyrosines by a combination of affinity preferences and cooperative interactions.

ACKNOWLEDGMENT

We thank Dr. C. Jane McGlade for providing the mouse Gads cDNA, Dr. Graham Carpenter for providing the rat PLC-γ1 cDNA, Dr. Leslie Berg for providing the human SLP-76 cDNA, and Dr. Tony Pawson for providing the Grb2 baculovirus. We also thank Dr. Sharlyn Mazur for help with manuscript preparation, Dr. John Ladbury and Dr. Stephen Bunnell for helpful comments, and Dr. Dong Xie for helpful advice.

REFERENCES

1. Burack, W. R., Cheng, A. M., and Shaw, A. S. (2002) Scaffolds, adaptors and linkers of TCR signaling: theory and practice, *Curr. Opin. Immunol. 14*, 312−316.
2. Pawson, T., Gish, G. D., and Nash, P. (2001) SH2 domains, interaction modules and cellular wiring, *Trends Cell Biol. 11*, 504−511.
3. Kuriyan, J., and Cowburn, D. (1997) Modular peptide recognition domains in eukaryotic signaling, *Annu. Rev. Biophys. Biomol. Struct. 26*, 259−288.
4. Schlessinger, J. (2000) Cell signaling by receptor tyrosine kinases, *Cell 103*, 211−225.

5. Ladbury, J. E., and Arold, S. (2000) Searching for specificity in SH domains, *Chem. Biol. 7*, R3−R8.
6. Kang, H., Freund, C., Duke-Cohan, J. S., Musacchio, A., Wagner, G., and Rudd, C. E. (2000) SH3 domain recognition of a proline-independent tyrosine-based RKxxYxxY motif in immune cell adaptor SKAP55, *EMBO J. 19*, 2889−2899.
7. Berry, D., Nash, P., Liu, S., Pawson, T., and McGlade, C. J. (2002) A high-affinity Arg-X-X-Lys SH3 binding motif confers specificity for the interaction between Gads and SLP-76 in T Cell signaling, *Curr. Biol. 12*, 1336.
8. Zhang, W., Sloan-Lancaster, J., Kitchen, J., Trible, R. P., and Samelson, L. E. (1998) LAT: the ZAP-70 tyrosine kinase substrate that links T cell receptor to cellular activation, *Cell 92*, 83−92.
9. Wange, R. L. (2000) LAT, the linker for activation of T cells: a bridge between T cell-specific and general signaling pathways, *Sci. STKE 2000*, RE1.
10. Samelson, L. E. (2002) Signal transduction mediated by the T cell antigen receptor: the role of adapter proteins, *Annu. Rev. Immunol. 20*, 371−394.
11. Zhu, M., Janssen, E., and Zhang, W. (2003) Minimal requirement of tyrosine residues on linker for activation of T cells in T cell activation and thymocyte development, *J. Immunol. 170*, 325−333.
12. Zhang, W., Trible, R. P., Zhu, M., Liu, S. K., McGlade, C. J., and Samelson, L. E. (2000) Association of Grb2, Gads, and phospholipase C-gamma 1 with phosphorylated LAT tyrosine residues. Effect of LAT tyrosine mutations on T cell angigen receptor-mediated signaling, *J. Biol. Chem. 275*, 23355−23361.
13. Lin, J., and Weiss, A. (2001) Identification of the minimal tyrosine residues required for linker for activation of T cell function, *J. Biol. Chem. 276*, 29588−29595.
14. Paz, P. E., Wang, S., Clarke, H., Lu, X., Stokoe, D., and Abo, A. (2001) Mapping the ZAP-70 phosphorylation sites on LAT (linker for activation of T cells) required for recruitment and activation of signalling proteins in T cells, *Biochem. J. 356*, 461−471.
15. Stoica, B., DeBell, K. E., Graham, L., Rellahan, B. L., Alava, M. A., Laborda, J., and Bonvini, E. (1998) The amino-terminal Src homology 2 domain of phospholipase C gamma 1 is essential for TCR-induced tyrosine phosphorylation of phospholipase C gamma 1, *J. Immunol. 160*, 1059−1066.
16. Irvin, B. J., Williams, B. L., Nilson, A. E., Maynor, H. O., and Abraham, R. T. (2000) Pleiotropic contributions of phospholipase C-gamma1 (PLC-gamma1) to T-cell antigen receptor-mediated signaling: reconstitution studies of a PLC-gamma1-deficient Jurkat T-cell line, *Mol. Cell. Biol. 20*, 9149−9161.
17. Yablonski, D., Kadlecek, T., and Weiss, A. (2001) Identification of a phospholipase C-gamma1 (PLC-gamma1) SH3 domain-binding site in SLP-76 required for T-cell receptor-mediated activation of PLC-gamma1 and NFAT, *Mol. Cell. Biol. 21*, 4208−4218.
18. Kurosaki, T., and Tsukada, S. (2000) BLNK: connecting syk and Btk to calcium signals, *Immunity 12*, 1−5.
19. Liu, Q., Berry, D., Nash, P., Pawson, T., McGlade, C. J., and Li, S. S. (2003) Structural basis for specific binding of the Gads SH3 domain to an RxxK motif-containing SLP-76 peptide: a novel mode of peptide recognition, *Mol. Cell 11*, 471−481.
20. Motto, D. G., Ross, S. E., Jackman, J. K., Sun, Q., Olson, A. L., Findell, P. R., and Koretzky, G. A. (1994) In vivo association of Grb2 with pp116, a substrate of the T cell antigen receptor-activated protein tyrosine kinase, *J. Biol. Chem. 269*, 21608−21613.
21. Wiseman, T., Williston, S., Brandts, J. F., and Lin, L. N. (1989) Rapid measurement of binding constants and heats of binding using a new titration calorimeter, *Anal. Biochem. 179*, 131−137.
22. Svedberg, T., and Pedersen, K. O. (1940) *The ultracentrifuge*, Oxford University Press, London.
23. Schuck, P., and Braswell, E. H. (2000) in *Current Protocols in Immunology* (Coligan, J. E., Kruisbeek, A. M., Margulies, D. H., Shevach, E. M., and Strober, W., Eds.) pp 18.8.1−18.8.22, John Wiley & Sons, New York.
24. Vistica, J., Dam, J., Balbo, A., Yikilmaz, E., Mariuzza, R. A., Rouault, T. A., and Schuck, P. (2004) Sedimentation equilibrium analyssi of protein interactions with global implicit mass conservation constraints and systematic noise decomposition, *Anal. Biochem.* (in press).
25. Schuck, P., Perugini, M. A., Gonzales, N. R., Howlett, G. J., and Schubert, D. (2002) Size-distribution analysis of proteins by analytical ultracentrifugation: Strategies and application to model systems, *Biophys. J. 82*, 1096−1111.
26. Lamm, O. (1929) Die differentialgleichung der ultrazentrifugierung, *Ark. Mater. Astr. Fys. 21B*, 1−4.
27. Schuck, P. (1998) Sedimentation analysis of noninteracting and self-associating solutes using numerical solutions to the Lamm equation, *Biophys. J. 75*, 1503−1512.
28. Dam, J., and Schuck, P. (2004) Calculating sedimentation coefficient distributions by direct modeling of sedimentation velocity profiles, *Methods Enzymol.* (in press).
29. Schuck, P., and Demeler, B. (1999) Direct sedimentation analysis of interference optical data in analytical ultracentrifugation, *Biophys. J. 76*, 2288−2296.
30. Lemmon, M. A., and Ladbury, J. E. (1994) Thermodynamic studies of tyrosyl-phosphopeptide binding to the SH2 domain of p56lck, *Biochemistry 33*, 5070−5076.
31. McNemar, C., Snow, M. E., Windsor, W. T., Prongay, A., Mui, P., Zhang, R., Durkin, J., Le, H. V., and Weber, P. C. (1997) Thermodynamic and structural analysis of phosphotyrosine polypeptide binding to Grb2-SH2, *Biochemistry 36*, 10006−10014.
32. Bradshaw, J. M., Grucza, R. A., Ladbury, J. E., and Waksman, G. (1998) Probing the "two-pronged plug two-holed socket" model for the mechanism of binding of the Src SH2 domain to phosphotyrosyl peptides: a thermodynamic study, *Biochemistry 37*, 9083−9090.
33. Ladbury, J. E., Hensmann, M., Panayotou, G., and Campbell, I. D. (1996) Alternative modes of tyrosyl phosphopeptide binding to a Src family SH2 domain: implications for regulation of tyrosine kinase activity, *Biochemistry 35*, 11062−11069.
34. O'Brien, R., Rugman, P., Renzoni, D., Layton, M., Handa, R., Hilyard, K., Waterfield, M. D., Driscoll, P. C., and Ladbury, J. E. (2000) Alternative modes of binding of proteins with tandem SH2 domains, *Protein Sci. 9*, 570−579.
35. Harkiolaki, M., Lewitzky, M., Gilbert, R. J., Jones, E. Y., Bourette, R. P., Mouchiroud, G., Sondermann, H., Moarefi, I., and Feller, S. M. (2003) Structural basis for SH3 domain-mediated high-affinity binding between Mona/Gads and SLP-76, *EMBO J. 22*, 2571−2582.
36. Sparks, A. B., Rider, J. E., Hoffman, N. G., Fowlkes, D. M., Quillam, L. A., and Kay, B. K. (1996) Distinct ligand preferences of Src homology 3 domains from Src, Yes, Abl, Cortactin, p53bp2, PLCgamma, Crk, and Grb2, *Proc. Natl. Acad. Sci. U.S.A. 93*, 1540−1544.
37. Drake, A. F. (2001) in *Protein−Ligand Interactions: Structure and Spectroscopy* (Harding, S. E., and Chowdhry, B. Z., Eds.) pp 123−167, Oxford University Press, Oxford.
38. Schuck, P. (2003) On the analysis of protein self-association by sedimentation velocity analytical ultracentrifugation, *Anal. Biochem 320*, 104−124.

BI0357311